CrystEngComm

ARTICLE

Two–component organic crystals without hydrogen bonding: structure and intermolecular interaction in bimolecular stacking

Valentina Colombo,[a] Leonardo Lo Presti*[,a,b] and Angelo Gavezzotti[a]

A survey of crystal structures including two organic compounds unable to form hydrogen bonding has been carried out using the Cambridge Structural Database. Such systems are common and numerous. Association modes mostly include stacking of flat systems, one of them usually being an aromatic hydrocarbon. "Alternate-ladder" (AL) and "slanted column" (SC) motifs occur most frequently; AL is somewhat prevalent in fluoroarene and pyromellitic dianhydride cocrystals, whereas SC occurs preferentially, but not exclusively, with quinones, nitrobenzene, TCNB and TCNQ coformers. Segregation of A and B chemical units in separate columns is very seldom observed, while A···B is the energetically dominating pair in a vast majority of cases. A stable network of stacked A···B units seems to be a strict requirement for observing cocrystallization, even more than an overall higher stability of the cocrystal with respect to its coformers. This highlights the central role of kinetics factors in determining the drive to stacking hetero–recognition. Energy dissection using the PIXEL scheme shows that dispersion energies play a dominant but not exclusive role. The interaction between flat organic systems is found to be a viable synthetic approach for cocrystallization, on the same footing as the more popular O–H···O, O–H···N and N–H···O hydrogen bonding. Some practical suggestions for the choice of the best coformers are provided.

Received 00th January 20xx,
Accepted 00th January 20xx

DOI: 10.1039/x0xx00000x

www.rsc.org/

1. Introduction

The deliberate synthesis of two–component organic crystals (co–crystals) mostly exploits some form of hydrogen bond (HB), in the common belief that such an interaction is the strongest and most directional among structure–determining ones, and hence the most predictable. A single O,N–H···O,N coupling stabilizes an organic molecular pair by 25–45 kJ mol^{-1},[1] a relevant part of the average lattice energy of a medium–size organic molecule (100–150 kJ mol^{-1}).[2–4] As expected, and confirmed by a previous survey,[5] such bonds regularly appear whenever their precursors are present in the interacting moieties, with few exceptions.

We analyze in this paper another kind of structure–driving bimolecular interaction, namely the coupling of flat–ring molecular moieties, that goes under the common name of π–stacking interaction. The denomination, implying that the interaction potential is dominated by the delocalized electron system, are not without challenge.[6] The stacking drive may have a more complex origin, including also polarization and net Coulombic interaction,[3] a typical example being arene – fluoroarene compounds.[7–13] A particular case are charge–transfer complexes (CTC), in which an electron–donor molecule interacts with an electron acceptor, with possible development in several cutting–edge research applications as light emitting diodes (OLED), organic (photo)conductors, ferroelectric and magnetoresistant materials.[14] Here aromatic hydrocarbon donors interact with acceptors such as tetracyanobenzene (TCNB), tetracyano ethylene (TCNE) or tetracyano quinodimethane (TCNQ).[15–23] Several other classes of compounds, like pyromellitic dianhydride (PMD), nitrobenzenes and quinones provide a significant population of non–HB cocrystals. There is in addition a rich literature on CTC which employ tetrathiafulvalene as the donor molecule,[24,25] not considered here due to the difficulty of dealing with sulfur electronic requests in out computational schemes.

The aim of this study is to clarify the physical nature of the interaction among flat–ring moieties in binary crystals. The basic material comes from a search in the Cambridge Structural Database[26] (CSD) of crystal structures of binary compounds in which neither of the coformers provides hydrogen donors, *i.e.* with neither NH nor OH H–bearing groups. Crystal packing motifs are evaluated on the basis of geometrical criteria like stacking separations and relative molecular orientations. Lattice energies are calculated in the approximate AA–CLP scheme[27] or in the PIXEL scheme.[28] Another source of information is the study of dimer formation and stabilization energies, with a subdivision into Coulombic–polarization and dispersion stabilizing terms.[28] For 53 binary systems for which both the cocrystal structure and those of the two coformers, the relative stability of the cocrystal with respect to individual coformers is

[a] *Dipartimento di Chimica, Università di Milano, via Venezian 21, 20133 Milano, Italy. Email: leonardo.lopresti@unimi.it*
[b] *Centre for Materials Crystallography, Århus University, Langelandsgade 140, 8000 Århus, Denmark*

† Electronic Supplementary Information (ESI) available: full Tables of average bond lengths and distribution curves, calculated bond energy profiles, principal component analysis. See DOI: 10.1039/x0xx00000x

estimated in terms of excess packing energy, PE_{exc}.[5] When this quantity is destabilizing one is faced with a possible influence of kinetic factors.

Non hydrogen–bonding molecular pairing is frequent and offers a viable synthetic opportunity. We also offer some suggestions as to the choice of the most promising coformers.

2. Methods

2.1 Crystal structure search

The CCDC software Conquest[29] was used, followed by several in–house filtering programs. The search required the presence of two organic chemical units, in a 1:1 stoichiometry for simplicity and without loss of generality, and the absence of OH or NH donor hydrogen atoms. Clathrates and solvates were excluded because the search is directed to deliberate hetero–aggregation between molecules of comparable size. Hydrogen atom coordinates were reset according to the usual[28] standards, to a C–H distance of 1.08 Å. A set of 122 cocrystals (the NOHB–ALL set) was used for geometrical considerations and general statistics. A subset of 53 cocrystals, (the NOHB–ENE set) was selected, with their separate coformers also determined structurally (Figure 1). Detail of compound names and CSD refcodes is in ESI, Tables S1 and S2.

2.2 Energy calculations and parameterizations

Crystal energies were calculated by the approximate AA–CLP scheme[27] for the broader set, and by the PIXEL procedure[28] for the NOHB–ENE set. Due to the large size of the molecules electron density grids were obtained[30] at the MP2/6–31G level (rather than the usual 6–31G**), and the grid condensation level *n* was set to 5 (rather than the usual 4), with a reduction of the computing load by about 75%. Test calculations show that the following constant ratios hold for lattice energies: E(*n*=4)/E(*n*=5) = 0.94, E(31G**)/E(31G) = 0.89; the overall damp factor E(31G**,4)/E(31G, 5) is then equal to 0.84. Energies and energy differences are thus magnified by about 20%. The atomic polarizability of fluorine in the CLP setup is 0.40 Å^3, which reproduces the experimental sublimation enthalpy of octafluoronaphthalene in the atom–atom formulation. In the PIXEL formulation this value was increased to 0.55 Å^3 to obtain the same satisfactory result. Fluorine parameterization is always problematic in semiempirical formulations.

Hexafluorobenzene crystallizes with one and a half molecule in the asymmetric unit (CSD refcode HFBENZ02, Z'=1.5).[31] This causes difficulties in PIXEL crystal calculations. Using a crystal structure generation module that works smoothly for rigid molecules (Clpoly, adapted and modified from previous versions[32] with use of the AA–CLP potential), a $P2_1/c$, Z' = 1/2 crystal structure for centrosymmetric hexafluorobenzene was generated, nearly identical to the experimental one in cell parameters, density and lattice energy (Table ESI S3) and given the pseudo–refcode HFBRES02. The crystal structure of perfluoronaphthalene (CSD refcode OFNAPH07) is disordered at room conditions[33] with two orientations of equal population. An acceptable crystal structure is obtained by retaining only one of the two orientations (pseudo–refcode OFNRES07). The lattice energy of these two computational crystal structures compares favorably with experimental heats of sublimation (Table ESI S3). They were used in all applications in place of experimental ones.

3. Results

3.1 Lattice energies and cocrystal stabilization

Let PE(AB) be the packing energy of the A–B cocrystal, that is the energy gained when one mole of dimers packs into the

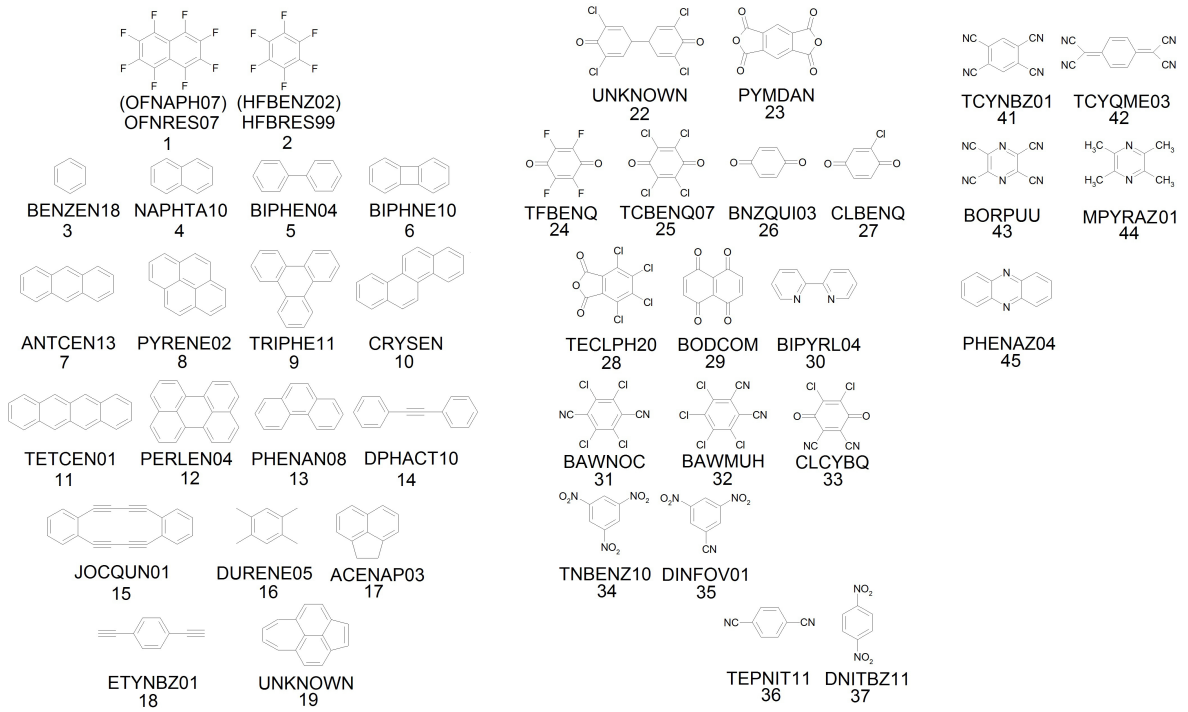

Figure 1. Coformers of the 53 cocrystals in the NOHB–ENE dataset. For each system, the molecular formula comes with the CSD refcode of the corresponding unary crystal and with an arbitrary numbering scheme. Any cocrystal in the NOHB–ENE dataset is unequivocally identified by the pair numbers of the corresponding coformers (see Sections 3.2ff below). The hexafluorobenzene and perfluoronaphthalene crystal structures (**1** and **2**) have been re–optimized (see text). The label 'UNKNOWN' marks those coformers (**19** and **22**) whose individual crystal structure is not included into the CSD.

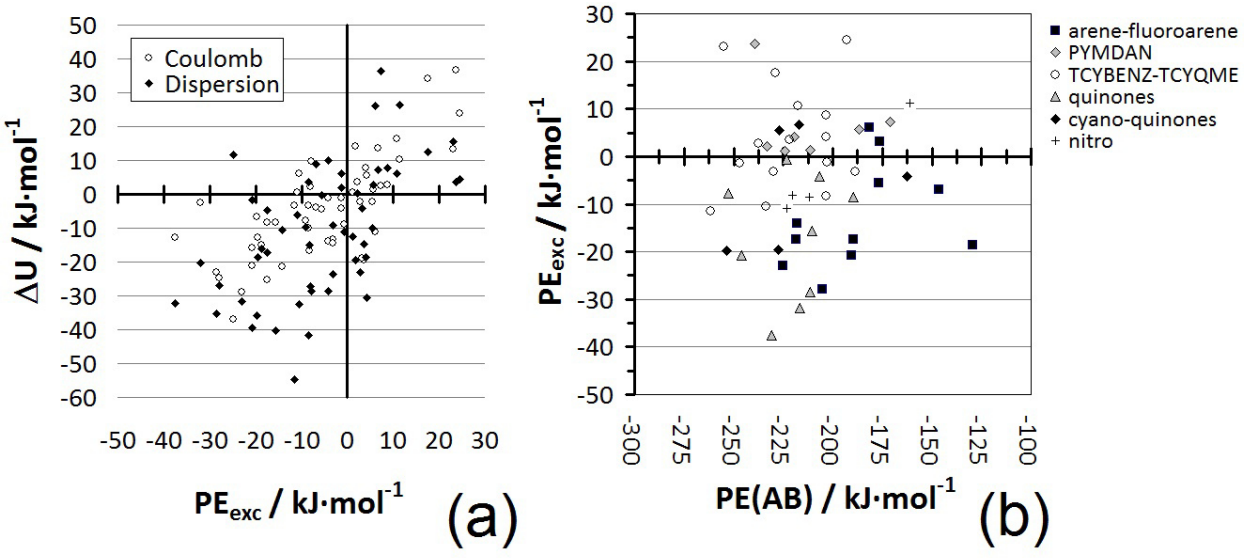

Figure 2. (a) Excess Coulombic (circles) and dispersion (rhombi) energies between cocrystal and sum of coformers, as a function of packing excess energy, for the NOHB–ENE dataset. (b) Packing excess energy as a function of total lattice energy of the cocrystal, PE(AB), for the same dataset. Different symbols highlight chemically different cocrystals (squares: arene–fluoroarene; crosses: NO_2–containing complexes; open circles: cocrystals involving compounds **41** or **42**; grey diamonds: cocrystals of compound **23**; black diamonds: cyano–quinones; triangles: quinones). See Figure 1 for the compound numbering.

crystal. Let PE(A) and PE(B) be the corresponding quantities for the two coformers. The difference between the internal lattice energy of the cocrystal and that of the separate coformers, ΔU_{exc}, is:

$$\Delta U_{\text{exc}} = \text{PE}_{\text{exc}} = \text{PE}(\text{AB}) - [\text{PE}(\text{A}) + \text{PE}(\text{B})] \quad (1)$$

According with a recent work by ourselves,[5] we refer to this quantity as the excess packing energy, PE_{exc}. When negative, it indicates stabilization of the binary system with respect to the separate components and invariably implies that more favorable (i.e. stronger, more extended) noncovalent interaction networks[5,34], are set up in the cocrystal with respect to either coformer. The intrinsic accuracy of the PIXEL method is of the order of a few kJ/mol, and such comparisons are made between crystal structures determined with different degrees of accuracy, introducing other minor uncertainties. Relying on previous experience,[5] an overall uncertainty threshold for energies is conservatively set at ±5 kJ/mol.

The results for the NOHB–ENE dataset are shown in Figure 2.The excess stabilization comes from a mix of Coulombic and dispersion factors, so that $PE_{exc} = \Delta U_{Coul} + \Delta U_{disp}$. 50% of the cocrystals are stabilized by more than 5 kJ/mol ($PE_{exc} << 0$), 27% are within the ±5 kJ/mol uncertainty zone ($PE_{exc} \sim 0$), while 23% are destabilized by more than 5 kJ/mol ($PE_{exc} >> 0$). However, very few net destabilizations exceed 10 kJ/mol. All considered, also recalling that differences are overestimated by about 20%, our conclusion here is that a significant thermodynamic excess stability results only in less than 50% of the cases. This estimate is slightly lower than that coming from 148 cocrystal PIXEL PE_{exc} evaluations of H–bonded cocrystal structures,[5] as ~ 55–56 % of them had $PE_{exc} << 0$. What is different is the distribution of cocrystals between the $PE_{exc} \sim 0$ and the $PE_{exc} >> 0$ groups, whose frequencies were as high as ~ 37% and ~7 % in the presence of hydrogen bonds.[5] The generation of a more favorable intermolecular network seems more likely with coformers having hydrogen bond ability than with non hydrogen bonding coformers. The present results comply well to very recent exprimental findings on the free energy differences between pharmaceutical cocrystals and pure component solids.[35]

3.2 Arene–perfluoroarene cocrystals

All structures contain strictly bound, flat and parallel A(fluoro)···B(hydrocarbon) dimers with interplanar separation of 3.3 to 3.7 Å. These dimers form infinite columns, which may then pack parallel, with a fluorinated entity in lateral contact with a hydrocarbon, the "alternate–ladder" (AL) packing mode (Figure 3a), or at an angle, the "slanted–columns" (SC) motif (Figure 3b) somewhat reminiscent of naphthalene packing.

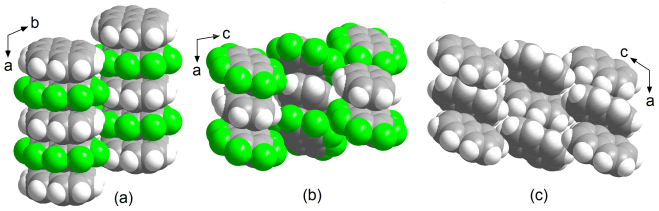

Figure 3. (a) The octafluoronaphthalene–pyrene (**1**:**8**) crystal (ECUVIH), model for the "alternate–ladder" packing motif and (b) the the octafluoronaphthalene–naphthalene (**1**:**4**) crystal (NPOFNP), model for the "slanted–columns" packing motif. For the sake of comparison, the packing of the unary naphtalene crystal (**4**, NAPHTA10), is shown in (c). Atoms are represented as van der Waals spheres according with standard chemical coloring scheme (C: grey, H: white, F: green). The unit cell reference system is also shown. Diamond v3.2k, (c) 1997–2014 Crystal Impact GbR, Bonn, Germany was employed throughout to draw molecular schemes.

These two motifs occur very frequently through the whole NOHB-ENE dataset (see below). AL is always associated with centric structures not exceeding the 2/m symmetry, whereas SC

is also found in polar space groups up to orthorhombic and tetragonal symmetry ($P2_1$: FOZHAD, PVVBFD01; $Pca2_1$, $Pna2_1$: PANCYIQ, VIGKIF; $P4_3$: PYRBZQ01). More complex packing arrangements, *i.e.* where relative tilting of adjacent pillars provides further degrees of freedom, generate more symmetry constraints. On the contrary, in AL-stacked systems pure translation is clearly important, while an inversion centre might arise from the intrinsic high point symmetry of the stacked coformers.

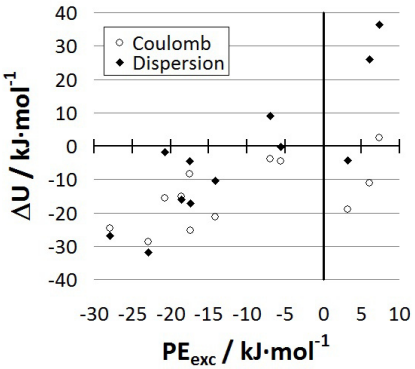

Figure 4. Coulombic (circles) and dispersive (rhombi) contributions to the packing excess energy (kJ mol^{-1}) in arene–fluoroarene cocrystals.

The excess energy of the arene-perfluoroarene cocrystal is almost invariably stabilizing (Figure 4), where dispersion and Coulombic energy cooperate on an almost equal footing. The exceptions are the perfluoronaphthalene cocrystal with acenaphthene (**1**:**17**), a non entirely planar coformer, and with diphenylacetylene (**1**:**14**); and the benzene–tetrayne (**3**:**15**) cocrystal. These destabilizing energies are anyway small and close to the significance threshold.

For perfluoronaphthalene, slanted column arrangements prevail with smaller coformers and alternate–ladder modes with larger coformers (Table 1). Introduction of perturbing non–planar methylene groups, as with acenaphthene and with 9,10–dihydrophenanthrene (VEHDIW), does not prevent the parallel–plane dimer stacking (if slightly distorted), but favors a sharply slanted–column arrangement. For hexafluorobenzene **2** the alternate–ladder mode is clearly preferred except in the cocrystal with the dibenzotetrayne **15**. One combined effect of these results seems to be that acetylenic (non condensed–ring) aromatics cocrystallize with more difficulty due to a large loss of stacking dispersion energy.

Table 1 shows the cohesive energies of single A···B pairs extracted from the crystal structure. As expected the dimers are held together by large dispersive contributions, but Coulomb–polarization terms are also important, possibly due to a stabilizing interaction between the opposite polarization of the C(–)–H(+) and C(+)–F(–) peripheral bonds. Dimer energies are higher for perfluoronaphthalenes than for perfluorobenzenes and increase as expected with the size of the coformer.

Many heavily fluorinated hydrocarbons give disordered or bad quality crystals, while unsubstituted hydrocarbons crystallize more easily. This is understandable considering that the chemical inertness of fluorinated compounds reflects in the intrinsic weakness of C–F···F and C–H···F contacts,[1,36,37] which in turn paves the way to a wealth of almost energetically equivalent packing modes. Hydrocarbons use parallel–stacking dispersive cohesion and T–shaped cohesion with mild stabilization and anyway lack of repulsion between C–H termini and π–electron clouds.

Table 1. Interplanar distances, R (Å), and dimerization energies (kJ·mol^{-1}) of stacked hetero–dimers extracted from the crystal structures of arene–fluoroarene cocrystals. See Figure 3 for an illustration of packing motifs and Figure 1 for the molecular formulae.

Coformer, number	CSD refcode	R[a]	E_{Coul}+ E_{pol}	E_{disp}	E_{tot}[b]	packing motifs[c]
Octafluoronaphthalene (**1**) cocrystals						
diphenylacetylene, **14**	OCAYIA	3.60	–26	–44	–39	SC
biphenyl, **5**	ASAKIO	3.68	–27	–49	–41	SC
biphenylene, **6**	ASAKOU	3.57	–32	–51	–42	AL
naphthalene, **4**	NPOFNP	3.73	–25	–46	–42	SC
acenaphthene, **17**	XUNJAR	3.60	–33	–58	–45	SC
		3.72	–32	–53	–45	
triphenylene, **9**	ECUVON	3.46	–36	–67	–52	AL
		3.42	–40	–72	–54	
anthracene, **7**	ECUTUR	3.41	–39	–67	–55	AL
pyrene, **8**	ECUVIH	3.36	–43	–79	–63	AL
hexafluorobenzene (**2**) cocrystals						
benzene, **3**	BICVUE01	3.76	–17	–23	–21	AL
DBCTDT,[d] **15**	JOCRIC01	3.71	–16	–33	–29	SC
naphthalene, **4**	IVOBOK	3.43	–24	–38	–34	AL
anthracene, **7**	ZZZGMW02	3.57	–27	–46	–36	AL
pyrene, **8**	ZZZGKE01	3.47	–26	–51	–44	AL

[a] Distance between centers of mass (includes a contribution from interplanar offset). [b] Difference between total (E_{tot}) and sum of Coulomb (E_{Coul}), polarization (E_{pol}) and dispersion (E_{disp}) is the repulsion energy. [c] SC: Slanted columns. AL: Alternate ladder. [d] Dibenzocyclododecadiene tetrayne.

Perfluoro compounds can use parallel stacking, but stacked columns cannot propagate into three–dimensional aggregates because lateral arrangement causes F···F repulsion; and T–shaped aggregation causes repulsion between C–F termini and π–clouds. The ease of formation of arene–fluoroarene cocrystals stems from favorable aggregation of lateral columns with proximity of C–H and C–F termini. This is sometimes considered a sort of C–H···F chemical bond. Given the very small involved interaction energies,[1,36] a safer view is probably to consider this arrangement rather a lack of repulsion than a stabilizing attraction.

3.3 Cocrystals of pyromellitic dianhydride (PMD) with polycyclic aromatics

Pyromellitic dianhydride (PMD, **23**) is a flat and strongly polar molecule. When co–crystallizing with polyciclic aromatics, the first three terms (Table 2) are isostructural forming A···B tightly stacked dimers and columns in an alternate–ladder (AL) packing (Figure 5a). The dimerization energy increases with increasing number of condensed rings. The chrysene and the biphenylene cocrystals (FILHIR, **10:23** and DURZAR01, **6:23**) show only partial molecular overlap in the dimers (Figure 5c–d). Contrary to the arene–perfluoroarene case, small coformers use the AL alternate–ladder motif while pyrene switches to the slanted–column (SC) type. All these facts point to a greater influence of Coulombic terms in these aggregates.

Dimer cohesion energies (Table 2) are always strongly stabilizing, both in dispersion and Coulombic terms. Excess lattice energies (Figure 2b and Table ESI S2) are mildly to strongly destabilizing, mostly due to loss of Coulombic–

polarization cohesion: in the tetracene cocrystal this loss is 23 kJ mol^{-1}. In its own crystal, the PMD molecule obtains strong Coulombic stabilization with negative anhydride oxygen regions pointing at the electron–depleted central ring. In the cocrystal the insertion of the non–polar hydrocarbon has the effect of a charge insulator. Kinetic effects due to stable dimer formation prior to crystallization might thus be at stake in overruling thermodynamic disadvantage.

Table 2. Interplanar distances, R (Å), and dimerization energies (kJ·mol^{-1}) of stacked hetero–dimers extracted from the crystal structures of PMD (**23**) cocrystals. See Figure 5 for definition of structure types and Figure 1 for the molecular formulae.

Coformer, Number	CSD refcode	R	E_{Coul}+ E_{pol}	E_{disp}	E_{tot}	packing motifs [a]
naphthalene,**4**	NAPYMA01	3.42	–38	–46	–45	AL
anthracene ,**7**	ANTPML	3.56	–48	–61	–49	AL
tetracene ,**11**	FILHOX	3.36	–43	–68	–55	AL
chrysene, **10**	FILHIR	3.87	–39	–54	–47	SC
biphenylene,**6**	DURZAR01	5.22 [b]	–16	–27	–19	NS
pyrene, **8**	PYRPMA02	3.65	–42	–63	–55	SC
phenazine , **45**	BECNUS10	3.60	–32	–50	–40	AL

[a] AL: Alternate-ladder motif; S: Slanted column motif; NS: Unusual non-stack motif. See Figure 5. [b] As the two molecules in the asymmetric unit are not parallel, an interplanar distance cannot be unequivocally defined and the centre of mass distance is given.

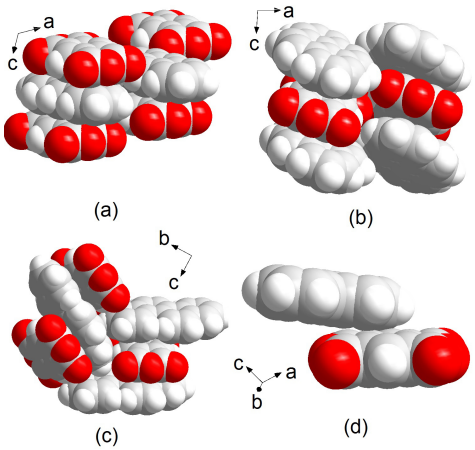

Figure 5. Cocrystals of PMD (**23**): (a) alternate–ladder (AL) with anthracene (ANTPML01, **7**), (b) slanted column (SC) with pyrene (PYRPMA02, **8**); (c) "Perpendicular ladder" (PL) motif: dimers have long molecular axes, roughly perpendicular with chrysene (FILHIR, **10**); (d) unusual non–stack NS dimerization mode with biphenylene, DURZAR01, **6**. Atoms are represented as van der Waals spheres (C: grey, H: white, O: red). The unit cell reference system is also shown.

3.4 Benzoquinones and carbonyl compounds with polycyclic aromatics.

Benzoquinones and halogenated carbonyl compounds **24–29** form a variety of cocrystals with polycyclic hydrocarbons, with a significant and consistent stabilization with respect to their coformers (Figure 6). Stabilization arises mainly from large dispersive contributions, but Coulombic terms are also not negligible. As in the hydrocarbon with fluorohydrocarbon case, alternation of halogenated and unsubstituted aromatics permits better interactions than either class of separate compounds.

The main packing motif consists of the usual infinite A···B···A···B columns, mostly in the slanted–column (SC) arrangement up to an extreme type in which the columns are nearly perpendicular to one another (CORPIJ **8**:**27** and PYRBZQ01 **8**:**26**, Figure ESI S1).

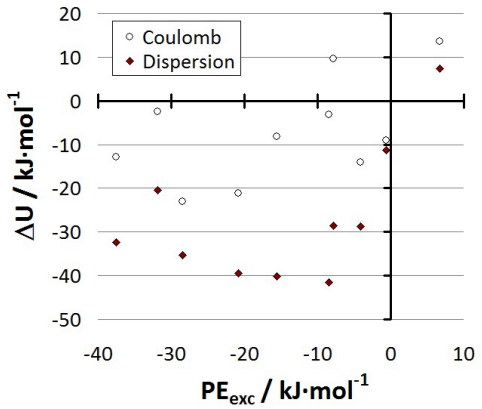

Figure 6. Coulombic (circles) and dispersive (rhombi) contributions to the packing excess energy (kJ mol^{-1}) in quinone and carbonyl compound cocrystals.

Dimerization energies (Table 3) increase with increasing size of the coformers (compare the pyrene **8** cocrystals with benzoquinone **26** and naphthalene tetrone **29**), but subtler Coulombic terms also play a role (compare pyrene: benzoquinone **26** with pyrene: fluoranil **24**). Chlorine substitution provides a larger dispersive contribution than fluorine, as expected from the respective atomic polarizabilities.

Table 3. Interplanar separation R (Å), and dimerization energies (kJ·mol^{-1}) of stacked hetero–dimers extracted from cocrystals of quinones and carbonyl compounds with hydrocarbons. See Figures 2 and 5 for the definition of structure types and Figure 1 for the molecular formulae.

Numbers, Coformers	CSD refcode	R	E_{Coul}+ E_{pol}	E_{disp}	E_{tot}	packing motifs [a]
8:26, pyrene : benzoquinone	PYRBZQ01	3.73	–16	–40	–27	SC (PL)
8: 27 pyrene : chlorobenzoquinone	CORPIJ	3.59	–20	–50	–35	SC (PL)
8: 29, pyrene : naphthalenetetrone	CEKBUP	3.66	–30	–58	–42	SC
8:**24**, pyrene : fluoranil	PYRFLR01	3.49	–47	–58	–51	SC
10: **24**, chrysene : fluoranil	CHRFAN	3.52	–38	–53	–46	SC
9: **24**, triphenylene : fluoranil	MOTRES	3.59	–34	–53	–46	SC
4: **28**, naphthalene : chloro phthalic anh.	DNPCPH	3.34	–44	–68	–49	AL
12: **25**, perylene : chloranil	CAFWAH	3.62	–42	–84	–55	AL
13: **28**, phenanthrene : chloro phthalic anh.	FOZHAD	3.53	–48	–84	–61	SC
7: **32**, anthracene : tetrachloro-1,2-dicyanobenzene	GOHYUZ	3.58	–33	–69	–55	AL

[a] AL: Alternate-ladder motif; SC: Slanted column motif; P: Perpendicular ladder motif. See Figures 3 and 5.

3.5 Nitrobenzene cocrystals

1,3,5–trinitrobenzene (**34**, TNB) and trinitrotoluene (TNT) are versatile coformers and coordinate a variety of companions: aromatic hydrocarbons, azines, thio compounds, etc. (see a list in Table ESI 4). In these cocrystals the TNB molecule is flat, while in the TNT molecule some nitro groups may be twisted out of plane. Tightly bound, flat A···B stacked dimers are formed (some are characterized in Table 4). TNB and TNT even form a cocrystal between themselves (NIBJUF), where however the molecules do not stack. The excess energies are in most cases slightly stabilizing (Figure 1b), with the exception of the 1,4–dinitrobenzene : diethynylbenzene cocrystal **37:18** (see below).

Table 4. Interplanar separation R (Å), and dimerization energies (kJ·mol^{-1}) of stacked hetero–dimers extracted from the structures of nitrobenzene cocrystals. See Figures 2 and 5 for the definition of structure types and Figure 1 for the molecular formulae, according to the numbering scheme.

Numbers, Coformers	CSD refcode	R	E_{Coul}+ E_{pol}	E_{disp}	E_{tot}	Motifs[a]
34: **9** TNB: triphenylene	PVVBFD01	3.58	–36	–59	–50	SC
34: **10**, TNB: Chrysene	VIGKIF	3.50	–38	–63	–57	SC
35: **8**, cyanodinitrobenz: pyrene	REDCIM	3.46	–37	–64	–55	AL
37: **38**, dinitrobenzene: diethynylbenz.	CECPEF	3.78 10.81 [b]	–12 –9	–31 –6	–26 –10[a]	SC

[a] AL: Alternate ladder motif; SC: Slanted column motif; See Figs. 3 and 5.
[b] Linear C–H···N dimer. Distance between centers of mass.

3.6 Tetracyanobenzene (TCNB) and tetracyanoquino dimethane (TCNQ) cocrystals

TCNB (**41**) coordinates hydrocarbon molecules by a twofold mechanism: (i) parallel A···B stack of aromatic rings, and (ii) lateral interaction between electron–poor hydrogen–atom regions and the electron–rich dicyano bay–area (Figure 7 and Table 5).

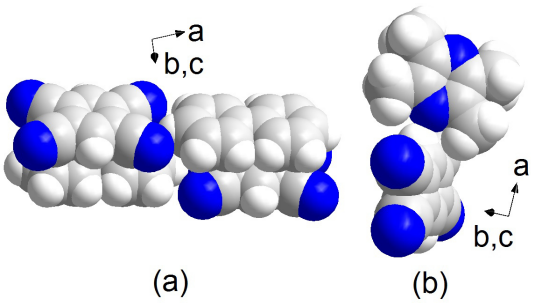

Figure 7. (a) A typical coordination mode for the TCNB (**41**):hydrocarbon cocrystals (here with biphenyl, refcode BUHSIG, **5**): ring stack and CH···NC bay–area contact. (b) The twisted configuration in the tetramethylpyrazine:TCNB (**44**:**41**) cocrystal (VERJUY01) with a short N···HC distance of 2.38 Å.

Cohesive energies of the stacked dimer are three to five times those of the lateral interaction involving the CH···N contacts; which is predominantly dispersive, a fact that is hardly reconciled with the definition of a CH···N bond. (I) and (ii) expand with the AL alternate–ladder motif (Fig. 7a). On the other hand, in the cocrystal with tetramethylpyrazine **44** (VERJUY01), the presence of methyl groups generates a twisted aggregation mode (TW, Figure 7b) that allows a contact between the acidic tetracyanobenzene hydrogen and the pyrazine nitrogen.

Table 5. Interplanar separation R (Å), and dimerization energies (kJ·mol^{-1}) of stacked hetero–dimers extracted from the crystal structures of TCNB (**41**) and TCNQ (**42**) cocrystals. The packing motif is alternate ladder (AL, Figures 2, 5 and 8) except for REHMUM, KARHAM and PYRTCQ02, for which it is slanted columns (SC, Fig. 8b), and VERJUI01 ("twisted" aggregation, Fig. 7b). See Fig. 1 for the molecular formulae.

Coformer, number	CSD refcode	R	E_{Coul}+ E_{pol}	E_{disp}	E_{tot}
TCNB (**41**) cocrystals					
anthracene, **7**	ANTCYB14	3.67 stack 10.3 CH···N[a]	–34 –10	–55 –10	–43 –10
biphenyl, **5**	BUHSIG	3.67 stack 9.87 CH···N	–23 –7	–38 –11	–38 –10
pyrene, **8**	PYRCBZ02[a]	3.58	–39	–61	–53
perylene, **12**	REHMUM	4.01	–26	–50	–45
diphenylacetylene, **14**	CIFWUJ	4.07	–24	–40	–37
tetramethyl pyrazine, **44**	VERJUY01	6.08	–33	–21	–34
tetramethylbenzene, **16**	KARHAM	3.76	–25	–42	–36
TCNQ (**42**) cocrystals					
naphthalene, **4**	TCQNAP01	3.90[a]	–26	–35	–45
chrysene, **10**	CHRTCQ01	3.58	–47	–82	–58
tetracene, **11**	HIGPUJ	3.59	–37	–72	–56
pyrene, **8**	PYRTCQ02	3.50	–40	–74	–58
DBCDT [b], **15**	JOCVEC01	3.56	–31	–61	–52
acenaphthene, **17**	ACNTCQ	3.85	–32	–53	–40
phenazine, **45**	TCQPEN10	4.29	–19	–45	–34

[a]Other CH···N cohesive interactions at 9 to 11 Å distance between centers of mass, and –8 to –15 kJ/mol.
[b] 1,2:7,8-Dibenzocyclododeca-1,7-diene-3,5,9,11-tetrayne

In cocrystals of TCNQ (**42**) the double–handle mechanism of A···B stack plus CH···NC bay–area interaction is present in almost all cases, and even survives the introduction of methyl groups that perturb the planarity of the coformer (Figure 8a). The alternate–ladder motif AL predominates except for the cocrystal with pyrene (**8**); due to the ovoidal shape of the hydrocarbon coformer (Figure 8b) the elongation axes are not strictly parallel, resulting in a slanted column SC motif.

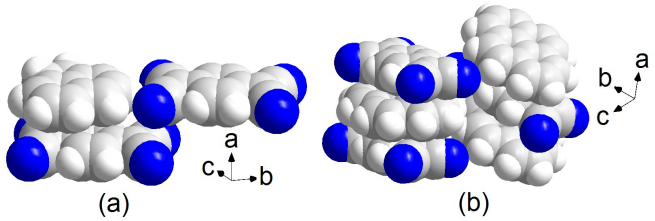

Figure 8. Packing modes in TCNQ (**42**) cocrystals. (a) The double–handle mechanism, with acenaphthene (**17**) (ACNTCQ), compare with Figure 7. (b) The slanted–column arrangement in the pyrene: TCNQ (**8:42**) cocrystal (PYRTCQ02).

In our calculations for TCNB (**41**) and even more TCNQ (**42**) nearly all complexes show very moderately stabilizing or actually destabilizing dispersive and Coulombic packing excess energies (Figure 9). Unless some energetic mechanism escaping our simulation is at work, a rationalization of the apparent

cocrystallization success must invoke some kinetic mechanism involving the capture of acidic Csp^2 hydrogens by the cyano embrace, followed by (or simultaneous with) stack buildup. A related key question concerns the yield of the cocrystallization reaction, which could be low as compatible with an unfavorable equilibrium.

3.7 Pyrene, ethynylbenzenes,methylated coformers

Pyrene (**8**) is one of the most versatile coformers in our sample. This molecule can cocrystallize with a variety of compounds of different chemical nature (Table S2, ESI), mostly with stabilizing excess energy (Figure ESI S2). The major component of stabilization is dispersion energy; the compact oval shape of pyrene apparently offers an accumulation of polarizable electrons and an ideal site for coupling in a π–stacking mode.

1,4–diethynylbenzene (**18**) forms cocrystals in which the acidic acetylenic hydrogen coordinates the nitrogen atom of aza-aromatics[38] (*i.e.* dipyridynes, RUXMAZ (**18**:**30**), nitriles (RUXMON (**18**:**36**)), and even nitro oxygens (CECPEF (**18**:**37**)); see ESI, Figure S3. In these systems, overlap of the aromatic rings is no longer a compelling option (Figure 10), while a T–shaped dimer (TS) and a CH···N dimer appear with comparable energies (Table 6). Here too, the cohesive energy of the CH···N dimer is 50% dispersive.

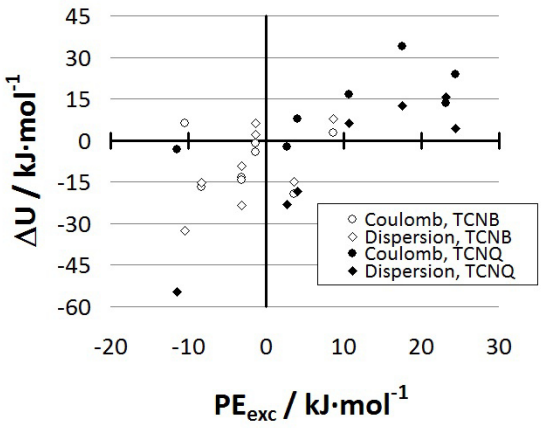

Figure 9. Coulombic (circles) and dispersive (rhombi) contributions to the packing excess energy (kJ·mol^{-1}) in cocrystals of TCNB (**41**, white symbols) and TCNQ (**42**, black symbols).

Table 6. Interplanar separation R (Å), and dimerization energies (kJ·mol^{-1}) of the main determinants in the crystal structures of diethynylbenzene (**18**) cocrystals, with T-shaped TS arrangement: stacked dimer and lateral CH···N interactions.

Coformer, number	CSD refcode	R	E_{Coul}+ E_{pol}	E_{disp}	E_{tot}
bipyridyl, **30**	RUXMAZ	4.63[a] 10.71[b]	–14 –38	–31 –10	–25 –21
dicyanobenzene, **36**	RUXMON	3.83 11.39	–10 –15	–30 –4	–20 –13

[a]Interplanar distances. [b]CH···N interaction, distances between centers of mass.

The introduction of methyl groups does not prevent the formation of tightly stacked dimers. For example, hexamethylbenzene forms cocrystals with the chloro cyanobenzenes **31** (ADULEQ03) and **32** (MOCCEM); durene **16** sticks to tetracyanobenzene **41** (KARHAM); 1,3,5–trimethylbenzene coordinates 1,3,5–tricyano–trichlorobenzene (NOKDAS) with methyl groups fitting below cyano groups. Methyl indentations may interlock with bulky chlorine substituents in a cogwheel fashion (CLAHMB02). TCNQ: phenazine **42**:**45** (TCQPEN) and TCNQ:N,N'–dimethylphenazine (TCQMHP) form identical dimers. A gallery of these examples is available as Figure ESI S4.

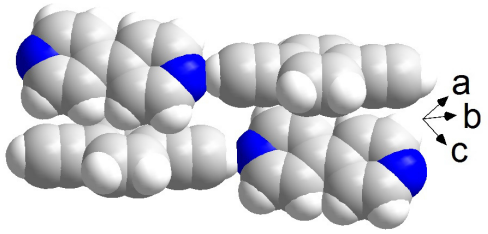

Figure 10. The 1,4–diethynylbenzene : 4,4'–bipyridyl cocrystal **18**:**30** (RUXMAZ): T–shaped dimer and CH···N bound dimer.

3.8 Hydrocarbon cocrystals?

Not considering benzene or toluene solvates, the CSD contains only one cocrystal between hydrocarbon molecules of comparable size, the benzene:biphenylacetylene **3**:**14** system (KURCEG; see Figure ESI S5). This structure features T–shaped (TS) arrangements with –C–H rims pointing to centers of neghbouring aromatic systems. The acetylene–benzene (ELIQUIZ) and acetylene–*m*–xylene (GURNIR) cocrystals have been obtained by an experimental *tour de force* from the liquids.[39] Acetylenic hydrogens point at the center of the benzene ring in a typical example of C–H···π interaction (Figure ESI S5).

One wonders whether cocrystallization between different flat–ring aromatic hydrocarbons has never been attempted (an unlikely case, since cocrystal research is an extremely active field), or is not viable. Mixtures of different aromatic hydrocarbons do not seem to find a driving force for hetero–crystallization. It would be instructive to see this hypothesis disproved by further experimental work, for example with the appearance of a cocrystal involving the most promising coformer, pyrene.

4. Relative importance of molecular pairs

A vital question in cocrystal chemistry is whether the A···B heterodimer is energetically predominant. If yes, a significant thermodynamic drive toward heterorecognition might be safely assumed, implying that strongly associated AB pairs might act as effective supramolecular synthons.[40,41] This is indeed the case for structures in the current NOHB-ENE dataset. Individual molecule–molecule pair energies were extracted from PIXEL lattice calculations and ranked according to their magnitude (highest to lowest). It turns out that the A···B heterodimer is 1st–ranking in 92 % and 2nd–ranking in 79 % of cases. Accordingly, A···A and B···B homodimers become dominant (66 %) only in the 3rd–ranking population. To the sake of comparison, the occurring frequencies of 1st– and 2nd–ranking A···B heteromolecular pairs in general hydrogen–bonded cocrystals[5] were respectively ~72 and ~56 %.

The sublattice energies due to all the A···A, B···B and A···B pairs in the crystal can be computed by the atom-atom CLP (AA-CLP) approach.[28] This method ignores many-body terms and is thus suitable for exactly partitioning the total lattice

energy into atomic, molecular and sublattice contributions. Though less accurate than PIXEL estimates, AA-CLP-based energies allow to disentangle, at least on relative grounds, what are the leading contributions to the overall cocrystal stability within any convenient molecule-based partition scheme. A "coupling energy" E_{cx} can be thus defined[5] as:

$$E_{cx} = E_t(AB) - 1/2\left[E_t(AA) + E_t(BB)\right] \quad (2)$$

E_t(XY), X, Y = A, B being the corresponding sublattice energies, as obtained by summing all the contributions of the symmetry-independent X···Y pairs in the crystal. Partition of E_{cx} (and so E_t(XY)) into electrostatic (E_{ce}), dispersion (E_{cd}) and repulsion (E_{cr}) terms is straightforward. Results for the NOHB-ALL dataset are shown in Figure 11.

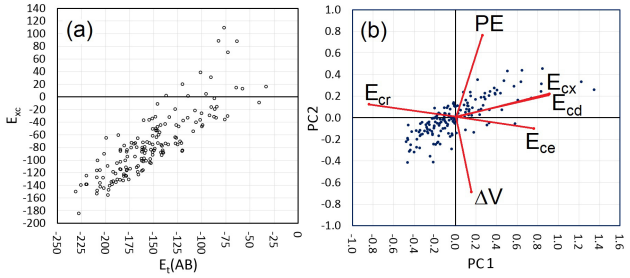

Figure 11. (a) Scatterplot of the coupling energy E_{cx} *vs* the AB sublattice packing energy. (b) Biplot of the variable loadings (red lines) and scores (blue dots) against the first (PC1, horizontal) and second (PC2, vertical) principal components. Scores were rescaled by a 0.1 factor. E_{ce}, E_{cd}, E_{cr} are electrostatic (Coulomb+polarization), dispersion and repulsion contributions to E_{cx}, PE is the packing energy and ΔV the A-B absolute molecular volume difference. Atom-atom, CLP-scheme energies on 160 binary crystals in the NOHB-ALL dataset. kJ·mol^{-1} units.

Similarly to what already pointed out for general hydrogen-bonded binary crystals,[5] a large majority (94 %) of structures have E_{cx} < 0 within our intrinsic uncertainty of 5 kJ·mol^{-1} (see above). This implies that lattice stability of NOHB cocrystals mainly relies on effectiveness of heteromolecular interactions. Structures with E_{cx} >> 0 are not able to set up strong favorable interactions involving both coformers.

Principal Component Analysis (PCA) allows one to identify what factors account for predominant data variability, sometimes helping in disclosing the underlying physics. The analysis was carried out as described elsewhere[42,43] on the whole NOHB-ALL dataset. Figure 11b shows the results; packing energy PE, E_{cx} E_{ce}, E_{cd} and E_{cr} define the variable space together with |ΔV|, the absolute difference between molecular volumes of A and B coformers. Original variables are represented as vector loadings, while the scores (blue dots) correspond to cocrystal coordinates in the reference frame of the new variables PC1 and PC2. The latter account for roughly 70 % of the data variance; according to the Kaiser-Guttman criterion,[44] no further principal components are significant. Full statistical information are available in the ESI (Tables S5–S8).

Here PC1 represents the covariance of coupling energy terms, whereas PC2 is mainly related to packing energy PE. A strong positive correlation exist between PE and |ΔV| (recall that they bear opposite sign), meaning that coformers with similar molecular volumes form cocrystals with less favorable PE. This might be explained considering that molecules of similar volume have also a similar shape, so a number of nearly isoenergetic approaching/packing modes among them exist, differing for example in the relative tilting of the polycondensed units. For this reason, hetero-recognition becomes statistically less probable, as without specific driving forces there is no reason for which the A···B interaction mode should be preferred over the A···A and B···B ones. On the contrary, when the two coformers significantly differ in size, a further constraint is added, namely the steric requirements of the larger unit. Thus, the presence of the smaller coformer in the neighbourhood of the larger one should become more probable, as the former is likely best suited to fit void spaces while producing favourable A···B interactions. This might provide a possible explanation for the lacking of cocrystals between hydrocarbon molecules of comparable size (Section 3.8 above). However, the scores follow the North-East/South-West direction, implying that their variability is mostly dominated by the coupling energy, E_{cx}, and not by PE. In turn, E_{cx} positively correlates with the dispersion term, E_{cd}, as their loadings are strongly superimposed. Finally, electrostatics (E_{ce}) plays a less important, though not negligible, role. Actually, it is known that cohesive contributions due to stacking interactions are partly electrostatic in nature,[3] as pointed out by the features of the electrostatic potential mapped onto the corresponding molecular Hirshfeld surfaces.[45,46]

5. Conclusions

1) Co–crystallization of organic molecules without hydrogen bonding is a viable synthetic approach. The common recipe involves flat aromatic hydrocarbons cocrystallizing with fluoroarenes, pyromellitic dianhydride, trinitrobenzenes, tetracyanoquino dimethane and tetracyanobenzene, halogenated quinones and other carbonyl compounds. The usual basic aggregation unit is a stacked dimer of planar or almost planar (methylated) chemical units, with a cohesive energy of 25–60 kJ mol^{-1}, comparable with that of a typical singly or doubly hydrogen–bonded pair.

2) Stacked planar dimers aggregate into A···B···A···B infinite columns, which in turn pack laterally in two modes, with column axes (a) parallel, generating lateral A···B coplanar contact (the alternate–ladder model, AL), or (b) at an angle, generating a twist angle between the molecular planes in adjacent columns (the slanted–column model, SC). In some cases the twist angle can be up to 90° (perpendicular column axes, generating a sort of "perpendicular ladder" motif PL as a limiting case of the SC one). Segregation of A and B chemical units in separate columns does not occur in the NOHB-ENE sample and it is seldom observed in the NOHB-ALL one (*e.g.* VAFWOP, Fig. S6 ESI). However, it is always associated to unfavorable coupling energies. This suggests that for a cocrystal to materialize there must be some strong thermodynamic and/or kinetic drive to stacking hetero–recognition. In addition, separate A···A and B···B columns involve only lateral A···B recognition, and our results show that any lateral linkage is energetically much less favorable than A···B stacking. The notable exception is the tetrathiafulvalene : tetracyanoquinodimethane salt–cocrystal (TTF-TCNQ)[47] that packs in slanted columns of the two separate coformers. Unfortunately, segregation is a desirable property because donor–acceptor stacking prevents charge mobility and causes the material to be an insulator.

3) The excess packing energy, the difference between the lattice energy of the cocrystal and the sum of the lattice energies of separate coformers, is stabilizing for arene–fluoroarene and

quinone–arene complexes, less so for TCNB, and destabilizing for TCNQ cocrystals and for cocrystals of diethynylbenzenes with direct CH···N or CH···O intermolecular contacts. Even with due account of the relative accuracy of our calculations, the trends are very specific and consistent: a gain in lattice energy is neither necessary nor sufficient to grant cocrystalllization. This points to a significant kinetic effect in the process. The requirements of equilibrium thermodynamics are met when the evolving system is homogeneous and free from concentration and temperature gradients. Cocrystallizing systems often originate under peculiar or extreme experimental conditions or from heterogeneous preparations. Even minor cohesion biases can steer the system to thermodynamically unpredictable conditions.

4) The fundamental A···B heterodimer is found to have the largest pair cohesion energy in 92 % of the 53 cocrystal structures within the NOHB-ENE dataset. In parallel and presumably not by chance, the total A···B contribution to the packing energy of the cocrystal also predominates on the total A···A and B···B ones in 94 % of cases. When hydrogen bonds are not available, a close and stable A···B association seems to be required, possibly already in the very early stage of nucleation, as top-ranking pairs are almost invariably heterodimers. Moreover, Principal Component Analysis points out that the stability of the resulting binary crystal crytically depends on the ability of the two coformers in setting up a stable network of stacked A···B units. This latter requirement seems to be even stricter than the need of a higher thermodynamic stability of the cocrystal with respect to its crystalline coformers (PE_{exc} << 0), further stressing the importance of kinetic effects in cocrystallization of flat hydrocarbons. In any case, the drive is mainly dispersive, with electrostatics playing a less central, but not negligible, role.

5) There are practically no examples of cocrystallization between unsubstituted hydrocarbons. The reasons are not clear; this could well be the result of scarce interest in what perhaps are not considered useful systems for applications. From the standpoint of a general theory of molecular recognition it would be useful to have a systematic exploration of this synthetic route. We suggest pyrene as one of the most versatile coformers and we would not be surprised if a pyrene–anthracene or pyrene–perylene cocrystal could be obtained.

Acknowledgements

V. C. and L. L. P. gratefully acknowledge economic support from Università degli Studi di Milano (Department of Chemistry) through the Development Plan for Atheneum grant (Action B, 2016-2017). L. L. P. also thanks DNRF for partial funding through the Centre for Materials Crystallography at Århus (DK) and the Italian supercomputing centre CINECA for the computational time provided through the CINECA-Unimi convention.

References

[1] A.Gavezzotti, *New J. Chem*. 2016, **40**, 6848–6853.

[2] W. J. Acree, Jr. and J. S. Chickos, *J. Phys. Chem. Ref. Data* 2010, **39**, 043101, 1–942.

[3] G. Macetti, L. Loconte, S. Rizzato, C. Gatti and L. Lo Presti, *Crystal Growth Des*. 2016, **16**, 6043–6054.

[4] A. Gavezzotti and L. Lo Presti, *Cryst. Growth Des*., 2015, **15**, 3792–3803.

[5] A. Gavezzotti, V. Colombo and L. Lo Presti, *Cryst. Growth Des.*, 2016, **16**, 6095–6104.

[6] C. R. Martinez and B. L. Iverson, *Chem. Sci.,* 2012, **3**, 2191–2201.

[7] J. C. Collings, K. P. Roscoe, R. Ll. Thomas, A. S. Batsanov, L. M. Stimson, J. A. K. Howard and T. B. Marder, *New J. Chem.* 2001, **25**, 1410–1417.

[8] J. C. Collings, K. P. Roscoe, E. G. Robins, A. S. Batsanov, L. M. Stimson, J. A. K. Howard, S. J. Clark and T. B. Marder, *New J. Chem.* 2002, **26**, 1740–1746.

[9] M. Gdaniec, W. Jankowski, M. J. Milewska and T. Połoński, *Angew.Chem*. 2003, **115**, 4033–4036.

[10] C. E. Smith, P. S. Smith, R. Ll. Thomas, E. G. Robins, J. C. Collings, C. Dai, A. J. Scott, S. Borwick, A. S. Batsanov, S. W. Watt, S. J. Clark, C. Viney, J. A. K. Howard, W. Clegg and T. B. Marder, *J. Mater. Chem*. 2004, **14**, 413–420.

[11] J. C. Collings, A. S. Batsanov, J. A. K. Howard and T. B. Marder, *Can. J. Chem*. 2006, **84**, 238–242.

[12] F. Cozzi, S. Bacchi, G. Filippini, T. Pilati and A. Gavezzotti, *Chem. Eur. J.* 2007, **13**, 7177–7184.

[13] F. Cozzi, S. Bacchi, G. Filippini, T. Pilati and A. Gavezzotti, *CrystEngComm* 2009, **11**, 1122–1127.

[14] K. P. Goetz, D. Vermeulen, M. E. Payne, C. Kloc, L. E. McNeil and O. D. Jurchescu, *J. Mater. Chem. C*, 2014, **2**, 3065–3076.

[15] A. Pawlukojć, W. Sawka–Dobrowolska G. Bator, L. Sobczyk, E. Grech, J. Nowicka–Scheibe, *Chem. Phys.* 2006, **327**, 311–318.

[16] X. Chi, C. Besnard, V. K. Thorsmølle, V. Y. Butko, A. J. Taylor, T. Siegrist and A. P. Ramirez, *Chem. Mater*. 2004, **16**, 5751–5755.

[17] M. A. Dobrowolski, G. Garbarino, M. Mezouar, A. Ciesielski and M. K. Cyrański, *CrystEngComm* 2014, **16**, 415–429.

[18] A. Arrais, E. Boccaleri, G. Croce, M. Milanesio, R. Orlando and E. Diana, *CrystEngComm* 2003, **5**, 388–394.

[19] Y. Imai, K. Kamon, S. Kido, T. Harada, N. Tajima, T. Sato, R. Kuroda and Y. Matsubara, *CrystEngComm* 2009, **11**, 620;

[20] S. Varughese, M. S. R. N. Kiran, U. Ramamurty, and G. R. Desiraju, *Chem. Asian J.* 2012, **7**, 2118–2125.

[21] T. Dahl, *Acta Crystallogr. Sect. C: Struct. Chem.* 2000, **C56**,708–710.

[22] T. Salzillo, M. Masino, G. Kociok–Köhn, D. Di Nuzzo, E. Venuti, R. G. Della Valle, D. Vanossi,
C. Fontanesi, A. Girlando, A. Brillante and E. Da Como, *Cryst. Growth Des*. 2016, **16**, 3028–3036.

[23] A. J. C. Buurma, O. D. Jurchescu, I. Shokaryev, J. Baas, A. Meetsma, G. A. de Wijs, R. A. de Groot and T. T. M. Palstra, *J. Phys. Chem. C* 2007, **111**, 3486–3489.

[24] P. Frère and P. J. Skabara, *Chem. Soc. Rev*. 2005, **34**, 69–98.

[25] N. Martín, *Chem. Comm*. 2013, **49**, 7025–7027.

[26] H. Allen, *Acta Crystallogr. Sect. B: Struct. Sci*. 2002, **B58**, 380−388.

[27] A. Gavezzotti, *New J. Chem*., 2011, **35**, 1360–1368.

[28] Deposited as Appendix I to: A. Gavezzotti, *Mol. Phys.* 2008, **106**, 1473–1485. Also available at http://www.angelogavezzotti.it, CLP link and documentation, current–pixel–theory.doc. Executables and source codes are freely available.

[29] I. J. Bruno, J. C. Cole, P. R. Edgington, M. Kessler, C. F. Macrae, P. McCabe, J. Pearson and R. Taylor, *Acta Crystallogr. Sect. B: Struct. Sci*. 2002, **58**, 389–397.

[30] Gaussian 03, Revision C.02, M. J. Frisch, G. W. Trucks, H. B. Schlegel, G. E. Scuseria, M. A. Robb, J. R. Cheeseman, J. A. Montgomery, Jr., T. Vreven, K. N. Kudin, J. C. Burant, J. M. Millam, S.

S. Iyengar, J. Tomasi, V. Barone, B. Mennucci, M. Cossi, G. Scalmani, N. Rega, G. A. Petersson, H. Nakatsuji, M. Hada, M. Ehara, K. Toyota, R. Fukuda, J. Hasegawa, M. Ishida, T. Nakajima, Y. Honda, O. Kitao, H. Nakai, M. Klene, X. Li, J. E. Knox, H. P. Hratchian, J. B. Cross, V. Bakken, C. Adamo, J. Jaramillo, R. Gomperts, R. E. Stratmann, O. Yazyev, A. J. Austin, R. Cammi, C. Pomelli, J. W. Ochterski, P. Y. Ayala, K. Morokuma, G. A. Voth, P. Salvador, J. J. Dannenberg, V. G. Zakrzewski, S. Dapprich, A. D. Daniels, M. C. Strain, O. Farkas, D. K. Malick, A. D. Rabuck, K. Raghavachari, J. B. Foresman, J. V. Ortiz, Q. Cui, A. G. Baboul, S. Clifford, J. Cioslowski, B. B. Stefanov, G. Liu, A. Liashenko, P. Piskorz, I. Komaromi, R. L. Martin, D. J. Fox, T. Keith, M. A. Al–Laham, C. Y. Peng, A. Nanayakkara, M. Challacombe, P. M. W. Gill, B. Johnson, W. Chen, M. W. Wong, C. Gonzalez and J. A. Pople, *Gaussian, Inc.*, Wallingford CT, 2004.

[31] H. Shorafa, D. Mollenhauer, B. Paulus, K. Seppelt, *Angew.Chem. Int. Ed.* 2009, **48**, 5845–5847.

[32] J. P. M. Lommerse, W. D. S.Motherwell, H. L. Ammon, J. D. Dunitz, A. Gavezzotti, D. W. M. Hofmann, F. J. J. Leusen, W. T. M. Mooij, S. L. Price, B. Schweizer, M. U. Schmidt, B. P. van Eijck, P. Verwer and D. E. Williams, *Acta Crystallogr. Sect. B: Struct. Sci*. 2000, **56**, 697–714.

[33] A. J. Ilott, S. Palucha, A. S. Batsanov, M. R. Wilson and P. Hodgkinson, *J. Am.Chem.Soc.* 2010, **132**, 5179–5185.

[34] G. Saleh, C. Gatti and L. Lo Presti, *Comput. Theor.Chem.*, 2015, **1053**, 53–59.

[35] C. A. Hunter and R. Prohens, *CrystEngComm*, 2017, **19**, 23–26.

[36] D. Chopra and T. N. Guru–Row, *CrystEngComm*, 2011, **13**, 2175–2186.

[37] L. Lo Presti, A. Ellern, R. Destro, R. Soave and B. Lunelli, *J. Phys. Chem. A* 2011, **115**, 12695-12707.

[38] This is also true for the tetrafluoro derivative of **18**, namely 1,4–diethynyl–2,3,5,6 tetrafluorobenzene–4,4'–ethyne ($C_{10}H_2F_4$, not included in our dataset). For example, see cocrystals with dipyridines with CSD refcodes FOJGOC and FOJGUI.

[39] R. Boese, T. Clark and A. Gavezzotti, *Helvetica Chim. Acta* 2003, **86**, 1085–1100.

[40] R. G. Desiraju, *J. Chem. Sci.* 2010, **122**, 667−675.

[41] L. Lo Presti, M. Sist, L. Loconte, A. Pinto, L. Tamborini and C. Gatti, *Crystal Growth Des*. 2014, **14**, 5822–5833.

[42] A. Gavezzotti and L. Lo Presti, *Crystal Growth Des*. 2016, 16, 2952−2962.

[43] R. Rakotomalala, TANAGRA: a free software for research and academic purposes. In Proceedings of EGC'2005, RNTI-E-3, 2005; Vol. 2, pp 697−702.

[44] H. F. Kaiser, *Psychological Reports* 1991, **68**, 855–858.

[45] M. A. Spackman and D. Jayatilaka, *CrystEngComm* 2009, **11**, 19–32.

[46] M. A. Spackman, J. J. McKinnon and D. Jayatilaka, *CrystEngComm* 2008, **10**, 377–388.

[47] U. Bernstein, P. M. Chaikin and P. Pincus, *Phys. Rev. Lett*. 1975, **34**, 271–274.

Table of Content Graphic

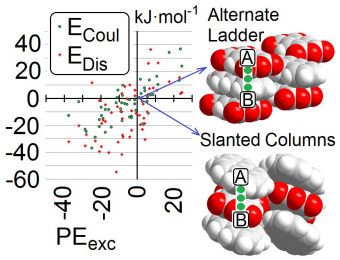

Synopsis TOC: Cocrystals of organic compounds unable to form hydrogen bonding are invariably stabilized by networks of π···π stacked A···B units. This requirement is even stricter than the need of a higher thermodynamic stability of the cocrystal with respect to its coformers.